JOURNAL OF MATERIALS SCIENCE 30 (1995) 5036–5041

Acicular ferrite transformation in deformed austenite of an alloy–steel weld metal

J. R. YANG, C. Y. HUANG, C. F. HUANG
Institute of Materials Science and Engineering, National Taiwan University, Taipei, Taiwan
J. H. AOH
Materials R and D Centre, Chung Shan Institute of Science and Technology, Taoyan, Taiwan

The effect of different amounts (5, 10 and 15%) of compressive deformation of austenite on the isothermal transformation of acicular ferrite in an alloy–steel weld metal has been investigated. It was found that prior deformation of austenite significantly enhanced acicular ferrite transformation. At the same isothermal transformation temperature, as a higher amount of prior deformation was applied, a greater quantity of acicular ferrite could be obtained and the size of acicular ferrite plates became much finer. These results implied that the effective nucleation sites of acicular ferrite increased with increasing amount of prior deformation. The other results also emphasized that the accumulated strain (due to prior deformation of austenite) could trigger acicular ferrite to nucleate on inclusions at high temperatures, where undeformed austenite remained stable. The acicular ferrite start temperature was found to be raised continuously by increasing the amount of prior deformation of austenite. Further evidence suggests that the application of deformation can boost the driving force for acicular ferrite formation. This phenomenon is similar to the case in which martensite forms under the influence of deformation.

1. Introduction

It is known that weld metals which possess good hardenability with respect to bainite consist mainly of acicular ferrite in the as-deposited condition [1]. The acicular ferrite plates form by a diffusionless and displacive transformation mechanism, and immediately after growth, carbon atoms are partitioned into the residual austenite. The transformation stops as the carbon concentration of austenite reaches the T'_0 curve. The experimental data [2–4] have clearly indicated that the transformation mechanism of acicular ferrite is essentially identical to that of bainite. The morphology of acicular ferrite differs from that of classical sheaf-like bainite because acicular ferrite nucleates intragranularly at inclusions within large austenite grains. After the initial nucleation event at inclusions, subsequent acicular ferrite plates can form sympathetically so that a one-to-one correspondence between the number of inclusions and the number of acicular ferrite plates is not expected. On the other hand, traditional bainite usually forms in wrought steels which have relatively small grains of prior austenite and are comparatively free of non-metallic inclusions. Bainite initially nucleates at prior austenite grain boundaries and continues growth by the repeated formation of subunits to generate the sheaf morphology. Acicular ferrite does not usually grow in sheaves because the development of sheaves can be stifled by hard impingement among plates nucleated independently at neighbouring sites. Recent research [5] has indicated that acicular ferrite and bainite can coexist, or exist separately in the same reheated weld metals. Acicular ferrite can form in the coarse-grained reheated weld metals, whereas bainite forms in the fine-grained reheated weld metals. However, in the medium-grained reheated weld metals, both acicular ferrite and bainite can be obtained; the volume fractions of bainite and acicular ferrite depend on the relative amounts of austenite grain surfaces and intragranular nucleation sites available.

The effect of stress on bainite transformation in alloy steels has been the object of much investigation [6–8] and has recently been the subject of an excellent review by Bhadeshia [9]. Because the bainite transformation occurs with the invariant-plane strain-shape deformation, the applied stress on the parent austenite phase would significantly influence the subsequent bainite transformation. Recent research [7, 8] has clearly shown that the external tensile stresses below the yield strength of austenite accelerate the bainite transformation. The elastic stresses tend to favour the development of certain crystallographic variants of bainite [8]. It has also been found that the acicular ferrite microstructure responds to compressive stresses below the yield strength of austenite [10]. The elastic stresses remarkably develop specific crystallographic variants and lead to a destruction of the conventional acicular

TABLE I Chemical composition (wt %) of alloy–steel weld metal

C	Si	Mn	Ni	Mo	Cr	V	S	P	Al	Ti	Nb	O	N
0.04	0.37	1.70	2.36	0.20	0.04	0.02	0.008	0.015	0.02	0.03	0.01	0.0370	0.0066

ferrite structure, where the ferrite plates emanating from inclusions point in many directions. When the applied stress exceeds the yield stress of the parent phase, the plastic deformation-induced defects might then influence the subsequent transformation behaviour. In this respect, there no related research for acicular ferrite has been reported. The purpose of the present work was to investigate the effect of different amounts of compressive deformation at a low austenite temperature on the acicular ferrite transformation in an alloy–steel weld metal.

2. Experimental procedure

The chemical composition of the weld metal studied is listed in Table I. The details of weld metal preparation by a manual metal arc (MMA) technique have been presented elsewhere [1]. The weld consisted of 21 runs with three runs per layer. The width of the weld was about 18 mm and the thickness of the parent plate 20 mm. For the purpose of investigating the effect of different amounts of prior compressive deformation on the acicular ferrite transformation, all the thermo-mechanical processes were performed in a Dilatromic III RDP deformation dilatometer of Theta Industries, Inc. The dilatometer has been interfaced to a computer work station PDP 11/55 central processor for analysing the resulting data. The software package (provided by Theta Industries, Inc.) can give a flexible and complete environment to execute the deformation and rapid cooling experiments. The length, time and temperature information can be recorded in microsecond intervals, and the level of vacuum can reach 10^{-5} torr to protect the oxidation of specimens.

Before preparation of dilatometric specimens, the pieces of the weld metal were homogenized at 1200 °C for 3 days while sealed in a quartz tube containing a partial pressure of pure argon. The specimens were machined in the form of 3 mm diameter cylindrical rods with 6 mm length. The scheme of the main thermo-mechanical processes carried out in dilatometer is given in Fig. 1. After reaustenitization at 1200 °C for 1 min, the samples were cooled to 700 °C at a cooling rate of 60 °C s^{-1}, and immediately, different amounts (5%, 10% and 15%) of compressive deformation were executed during cooling from 700 °C to 600 °C at the same cooling rate 60 °C s^{-1}, and then the deformed specimens were cooled directly to different isothermal temperatures. After the isothermal transformations were completed, the samples were quenched at 200 °C s^{-1} to the ambient temperature. The thermal treatments for undeformed specimens were identical to those of Fig. 1 without deformation being applied in the temperature range 700–600 °C.

The specimens for optical metallography were prepared from dilatometric specimens. The observed section was perpendicular to the direction of compression for the deformed samples. The specimens were mechanically polished and then etched in 20% nital solution. Transmission electron microscopy specimens were prepared from 0.25 mm thick discs sliced from dilatometric specimens. For the deformed samples, the observed section was perpendicular to the direction of compression. The discs were thinned to 0.05 mm by abrasion on silicon carbide paper and then twin-jet electropolished using a mixture of 5% perchloric acid, 25% glycerol and 70% ethanol at ambient temperature and 60 V polishing potential. They were examined using a Jeol 100CX transmission electron microscope operating at 100 kV.

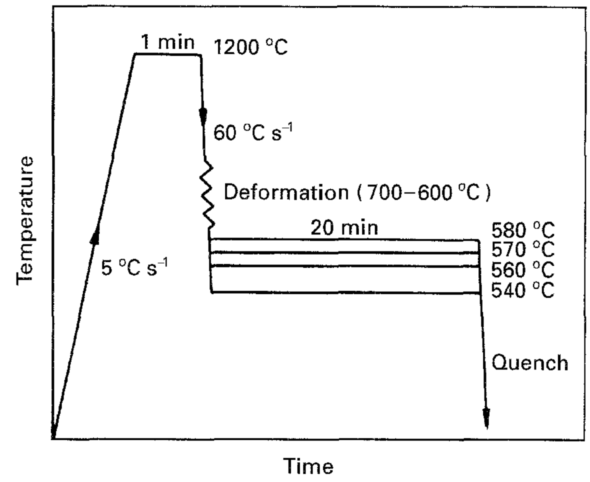

Figure 1 Schematic diagram showing the main thermo-mechanical processes performed in the dilatometer.

3. Results and discussion

The isothermal dilatometric curves for undeformed specimens (as presented in Fig. 2) indicate that the

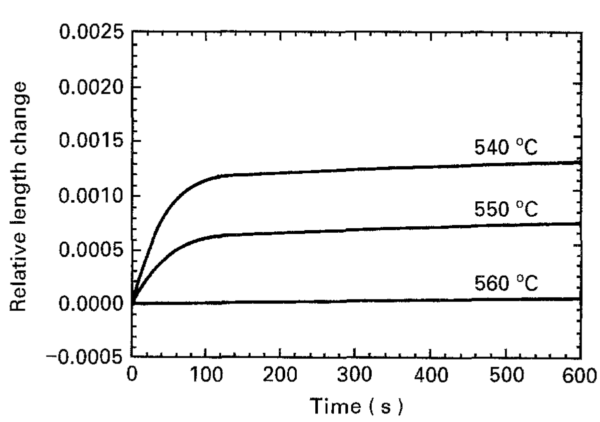

Figure 2 Dilatometric curves for the undeformed samples isothermally treated at 540, 550 and 560 °C.

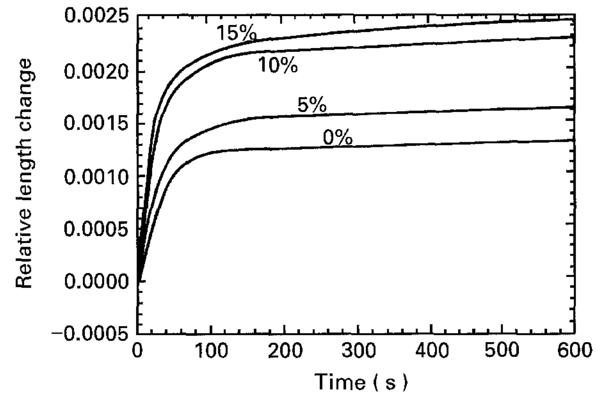

Figure 3 Dilatometric curves for isothermal treatments at 540 °C without and with prior deformation (the amounts of prior deformation are indicated).

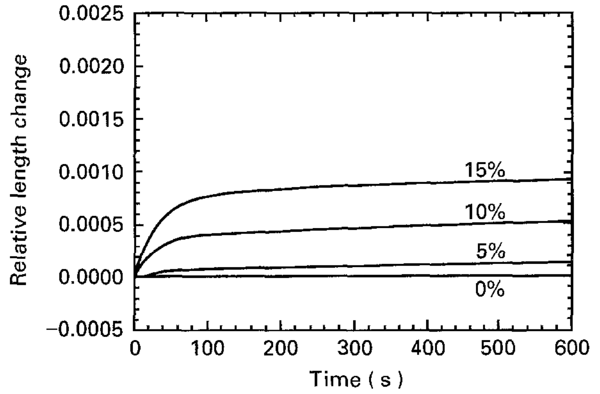

Figure 4 Dilatometric curves for isothermal treatments at 560 °C without and with prior deformation (the amounts of prior deformation are indicated).

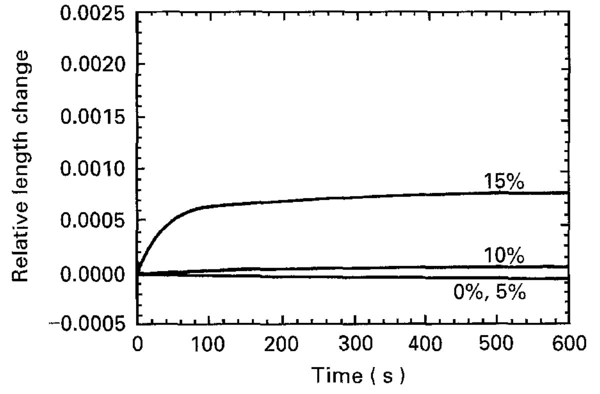

Figure 5 Dilatometric curves for isothermal treatments at 570 °C without and with prior deformation (the amounts of prior deformation are indicated).

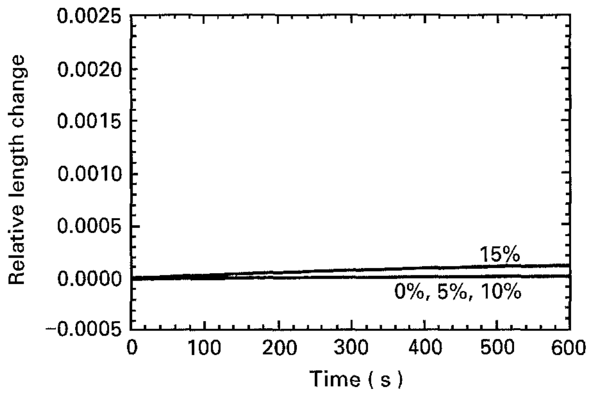

Figure 6 Dilatometric curves for isothermal treatments at 580 °C without and with prior deformation (the amounts of prior deformation are indicated).

maximum amount of transformation increases as the isothermal temperature decreases below 560 °C. It is apparent that the acicular ferrite start temperature is close to 560 °C. In order to elucidate the effect of prior compressive deformation of austenite on acicular ferrite transformation, the isothermal treatments for the deformed samples were therefore chosen at 540, 560, 570 and 580 °C, respectively, as shown in Fig. 1. The dilatometric curves (for different isothermal transformation temperatures) obtained from the samples with different amounts of deformation are shown in Figs 3–6. Fig. 3 shows that at 540 °C isothermal temperature, the maximum degree of transformation increases with increasing amount of compressive deformation. The corresponding optical micrographs in Fig. 7 illustrate the microstructures obtained from the dilatometric specimens (without and with different amounts of deformation) after completion of isothermal transformation at 540 °C, followed by rapid quenching to ambient temperature. The metallographs are consistent with the dilatometric results, and indicate that the volume fraction of acicular ferrite increases with increasing amount of deformation accordingly. It is also notable that the size of the acicular ferrite plate (as shown in Fig. 7) becomes smaller in the sample with the higher amount of deformation. The microstructural evidence implies that the higher amount of compressive deformation significantly enhances the effective nucleation sites for acicular ferrite formation. The dilatometric curves in Fig. 4 show that the acicular ferrite transformation can be clearly detected at 560 °C as the amount of compressive deformation reaches 5%. Fig. 8 presents the optical micrographs for the corresponding isothermal dilatometric data in Fig. 4 after acicular ferrite transformation has finished. The results also show that the compressive deformation promotes the acicular ferrite transformation; the higher the amount of deformation, the greater the quantity of acicular ferrite transformation.

The dilatometric curves in Fig. 5 show that the acicular ferrite can form at 570 °C if the amount of compressive deformation reaches 10%. Furthermore, the dilatometric curves in Fig. 6 indicate that the acicular ferrite transformation can be detected even at 580 °C when the amount of compressive deformation reaches 15%. It is apparent that the highest temperature at which acicular ferrite forms during cooling of austenite can be raised by the application of a suitable amount of deformation. This phenomenon is analogous to the case in which the martensite forms under the influence of deformation [11, 12]. For the latter case, the maximum temperature is well known as M_d. The deformation-induced martensitic transformation has been classified two modes, i.e. stress-assisted martensite and strain-induced martensite, based on the origin of nucleation sites that initiate

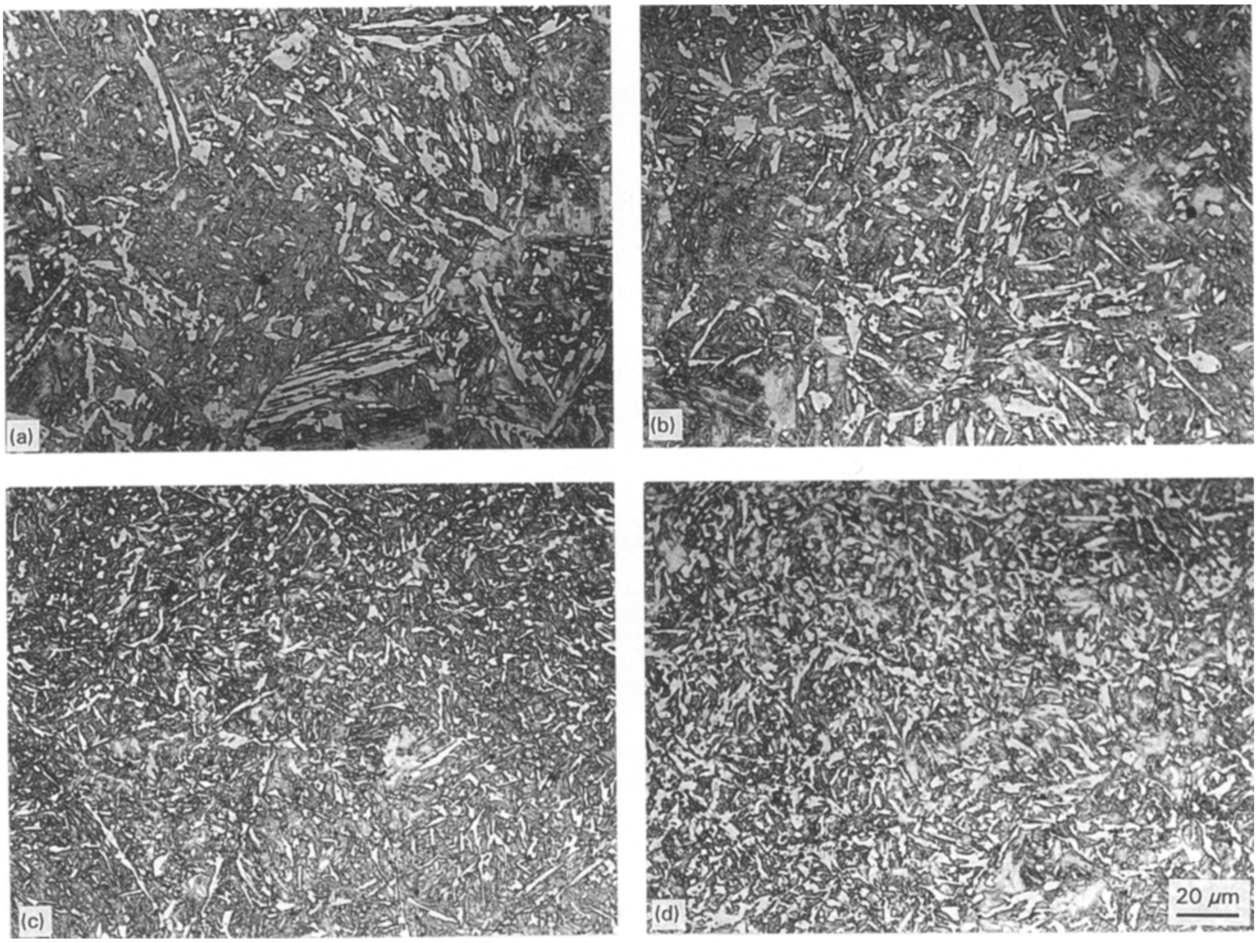

Figure 7 Optical metallographs showing the microstructures obtained from the dilatometric specimens isothermally treated at 540 °C for 20 min with different amounts of prior deformation: (a) 0%, (b) 5%, (c) 10% and (d) 15%.

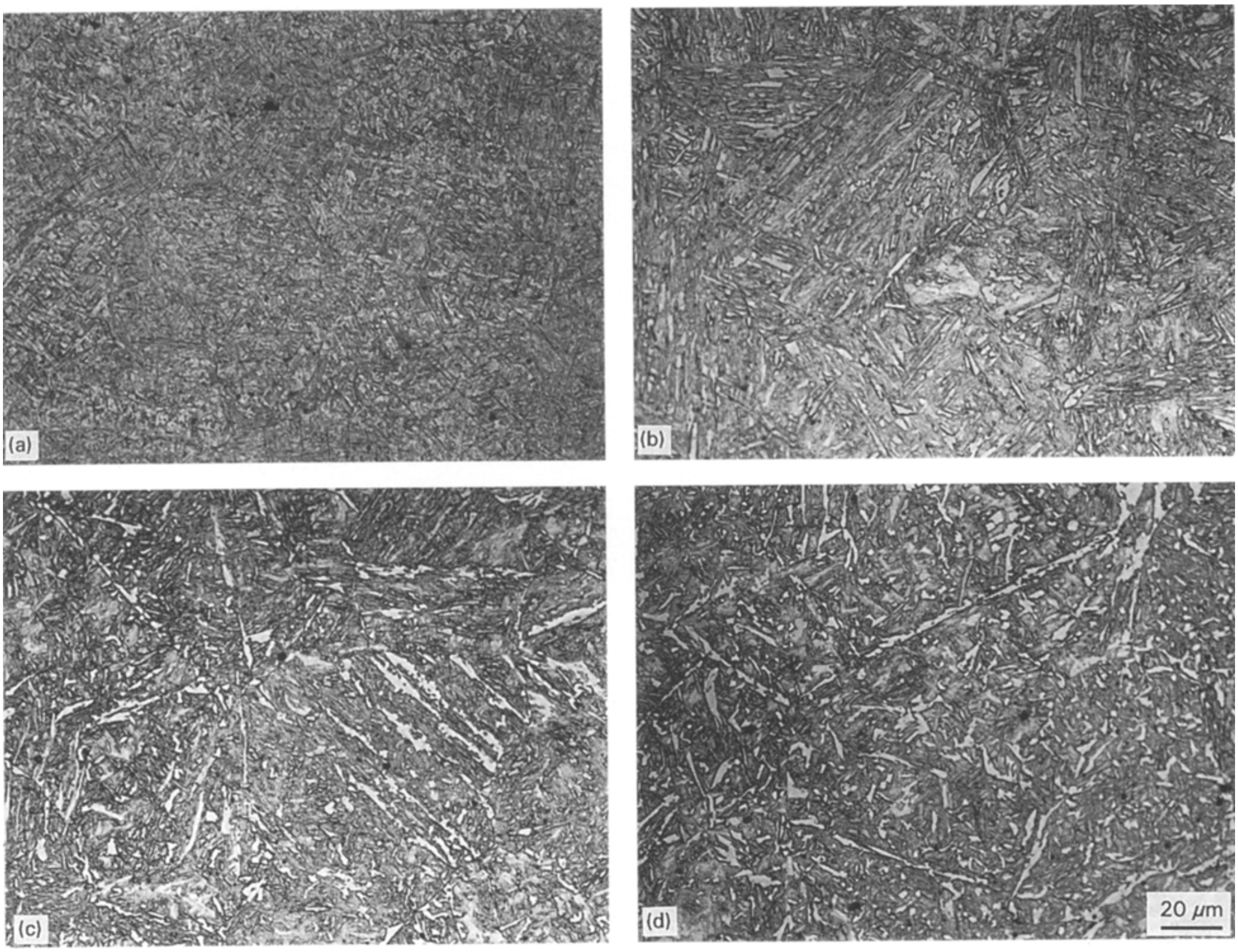

Figure 9 Transmission electron micrograph showing the microstructural details of the specimen with 15% deformation of austenite at 700 °C followed by isothermal transformation at 540 °C for 10 min.

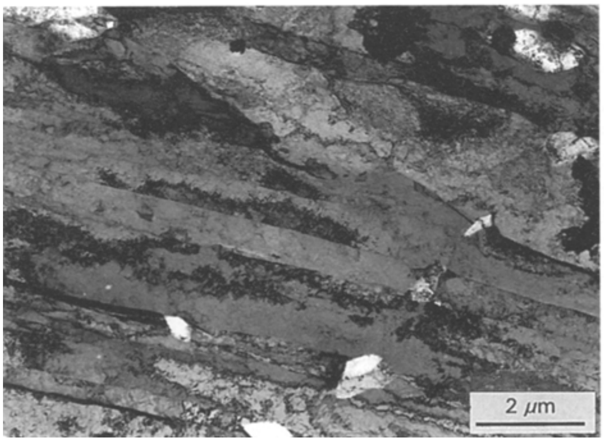

Figure 10 Transmission electron micrograph illustrating the acicular ferrite nucleation observed for the specimen with 10% deformation of austenite at 700 °C followed by isothermal transformation at 570 °C for 10 min. (The matrix austenite was transformed to martensite plates during rapid cooling to room temperature.)

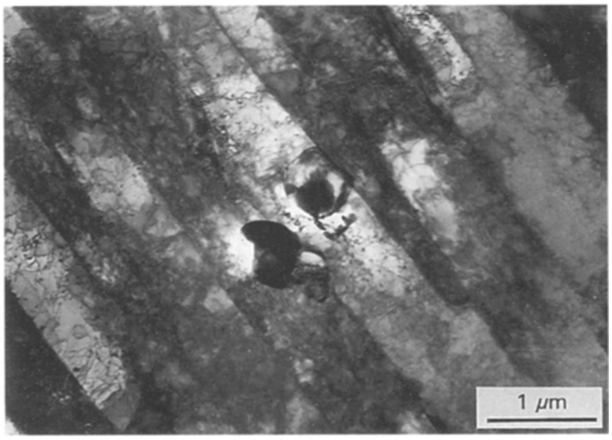

Figure 11 Transmission electron micrograph revealing the nucleation of acicular ferrite platelet on an inclusion even for the specimen with 15% deformation of austenite at 700 °C followed by isothermal transformation at 580 °C for 10 min. (The matrix austenite was transformed to martensite plates during rapid cooling to room temperature.)

the transformation. In stress-assisted martensite, nucleation on the pre-existing nucleation sites is assisted thermodynamically by externally applied stress. On the other hand, strain-induced martensite is based on the assumption that new nucleation sites are created by the substantial plastic deformation. As the oxygen content of the weld metal studied was 370 p.p.m., the quantities of inclusions in the weld metal would be significant. In this work, the prior compressive deformation of austenite would accumulate some amount of plastic strain in the vicinity of the inclusion/austenite matrix interface. Fig. 9 shows a transmission electron micrograph of the microstructure obtained from the sample with 15% deformation at 700 °C followed by isothermal transformation at 540 °C for 10 min. The microstructural character of acicular ferrite is clearly seen, but it cannot provide any evidence to show the trace of effective sites for strain-induced nucleation because the amount of acicular ferrite transformation was large at 540 °C. However, Fig. 10 shows a transmission electron micrograph of the acicular ferrite nuclea-

Figure 8 Optical metallographs showing the microstructures obtained from the dilatometric specimens isothermally treated at 560 °C for 20 min with different amounts of prior deformation: (a) 0%, (b) 5%, (c) 10% and (d) 15%.

tion observed after the specimen was given a 10% compressive deformation at 700 °C and then isothermally transformed at 570 °C. Moreover, the transmission electron micrograph in Fig. 11 shows that acicular ferrite nucleation can still be found after the sample was subjected to a 15% deformation at 700 °C and then isothermally transformed at 580 °C. The evidence implies that the accumulated strain can trigger acicular ferrite to nucleate on inclusions at high transformation temperatures, where the undeformed austenite remains stable. It is proposed that the application of compressive deformation can boost the driving force for acicular ferrite formation. Consequently, the acicular ferrite start temperature is raised continuously by increasing the amount of deformation.

4. Conclusions

1. Prior deformation of austenite significantly enhances the isothermal transformation of acicular ferrite. At the same isothermal temperatures, the volume fraction of acicular ferrite obtained increases with increasing amount of prior deformation; the size of the acicular ferrite plates becomes smaller in the specimen with the higher amount of deformation. It is apparent that the higher amount of compressive deformation increases the effective nucleation sites for acicular ferrite formation.

2. The highest temperature at which isothermal transformation of acicular ferrite occurs can be raised by increasing the amount of prior deformation of austenite. The evidence from transmission electron micrographs reveals that the accumulated strain triggers acicular ferrite to nucleate on inclusions at the higher transformation temperatures. It is suggested that the application of compressive deformation can boost the driving force for acicular ferrite formation; therefore, the acicular ferrite start temperatures rises continuously with increasing amount of prior deformation.

Acknowledgements

This work was carried out with financial support from the National Science Council of the Republic of China, Taiwan, under Contract NSC 83-0405-E-002-010. The authors thank Dr H. K. D. H. Bhadeshia for the supply of the weld metal.

References

1. J. R. YANG and H. K. D. H. BHADESHIA, *J. Mater. Sci.* **26** (1991) 839.
2. H. K. D. H. BHADESHIA and J. W. CHRISTIAN, *Metall. Trans.* **21A** (1990) 767.
3. J. R. YANG and H. K. D. H. BHADESHIA, in "Advances in Welding Science and Technology", edited by S. A. David (ASM, Cleveland, OH, 1987) p. 187.
4. M. STRANGWOOD and H. K. D. H. BHADESHIA. *ibid.*, 209.
5. J. R. YANG, C. Y. HUANG, C. F. HUANG and J. N. AOH, *J. Mater. Sci. Lett.* **11** (1992) 1547.
6. R. FREIWILLING, J. KUDRMAN and P. CHRASKA, *Metall. Trans.* **7A** (1976) 1091.
7. M. UMEMOTO, S. BANDO and I. TAMURA, in "Proceedings of the International Conference on Martensitic Transformations (ICOMAT'86)" (Japan Institute of Metals, 1986) p. 595.
8. H. K. D. H. BHADESHIA, S. A. DAVID, J. M. VITEK and R. W. REED, *Mater. Sci. Technol.* **7** (1991) 686.
9. H. K. D. H. BHADESHIA, "Bainite in Steels" (Institute of Materials, London, 1992) p. 210.
10. S. S. BABU and H. K. D. H. BHADESHIA, *Mater. Sci. Eng.* **A156** (1992) 1.
11. G. B. OLSON, in "Encyclopedia of Materials Science and Engineering", edited by R. W. Cahn (Pergamon, Oxford, 1986) p. 2929.
12. C. M. WAYMAN, in "Physical Metallurgy", edited by R. W. Cahn and P. Haasen (North-Holland, Amsterdam, 1983) p. 1031.

Received 14 February 1994
and accepted 11 April 1995